

# Measurement of the response function and the detection efficiency of an organic liquid scintillator for neutrons between 1 and 30 MeV

HUANG Han-Xiong(黄翰雄)<sup>1)</sup> RUAN Xi-Chao(阮锡超) CHEN Guo-Chang(陈国长)

ZHOU Zu-Ying(周祖英) LI Xia(李霞) BAO Jie(鲍杰)

NIE Yang-Bo(聂阳波) ZHONG Qi-Ping(仲启平)

(Department of Nuclear Physics, China Institute of Atomic Energy, Beijing 102413, China)

**Abstract** The light output function of a  $\phi 50.8 \text{ mm} \times 50.8 \text{ mm}$  BC501A scintillation detector was measured in the neutron energy region of 1 to 30 MeV by fitting the pulse height (PH) spectra for neutrons with the simulations from the NRESP code at the edge range. Using the new light output function, the neutron detection efficiency was determined with two Monte-Carlo codes, NEFF and SCINFUL. The calculated efficiency was corrected by comparing the simulated PH spectra with the measured ones. The determined efficiency was verified at the near threshold region and normalized with a Proton-Recoil-Telescope (PRT) at the 8—14 MeV energy region.

**Key words** liquid scintillator, response function, detection efficiency, Monte-Carlo, TOF

**PACS** 29.40.Mc

## 1 Introduction

Organic liquid scintillators (LS) are widely used in radiation detection because of their fast time response, high detection efficiency and the property of good Pulse-Shape Discrimination (PSD). Therefore its light output response to charged particles (i.e. electron, proton, alpha, and so on) is very important not only for nuclear physics research and the application of nuclear technology, but also for the study of the scintillator's luminescence mechanism. If the light output function of a detector and the exact reaction cross sections are precisely known, the detection efficiency of a detector can be determined very well by a Monte-Carlo (MC) simulation.

A lot of work on the efficiency calibration of a liquid scintillation detector have been done in the past, but much of this has focused on the neutron energy below 20 MeV. In the energy region above 20 MeV, contributions from the n-C reactions in the liquid scintillator become more and more important, while the reaction cross sections and the angular distributions are not precise enough. A little efficiency

calibration work above the 20 MeV region has been reported<sup>[1—5]</sup>. However, their results can not be used directly since the size of the detector and the detection threshold are different, even the composition of the scintillator is slightly different. Therefore, it is necessary to perform a precise calibration for our own detector.

In this paper, a precise neutron detection efficiency calibration was performed and calculations of two MC codes (NEFF and SCINFUL<sup>[6]</sup>) were compared with the measured results. The detection efficiency of a  $\phi 50.8 \text{ mm} \times 50.8 \text{ mm}$  BC501A liquid scintillation detector was obtained within the energy region of 1—30 MeV. The  $^{12}\text{C}(n, 3\alpha)$  reaction cross sections which have been used in the NEFF and NRESP<sup>[7]</sup> codes were improved according to the differences between the simulated and measured pulse height (PH) spectra.

## 2 Experiment

The experiment was carried out with the fast neutron Time-of-Flight (TOF) spectrometer at the HI-13 Tandem Accelerator at the China Institute of

Received 22 November 2008

1) E-mail: shawn@ciae.ac.cn

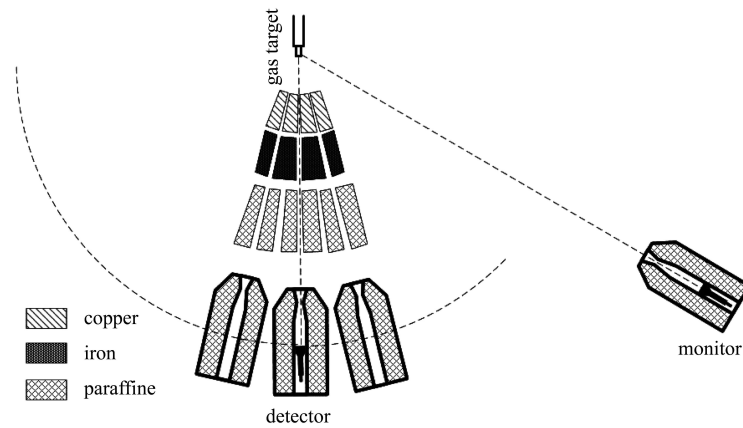


Fig. 1. The scheme of the fast neutron TOF spectrometer at CIAE.

Atomic Energy (CIAE). The schematic diagram of the spectrometer is shown in Fig. 1. More details can be found in Ref. [8].

The neutron detector was placed in the No.2 spectrometer (the middle one) at a distance 6.67 m from the gas target. The neutron flux was monitored by a  $\phi 30.0 \text{ mm} \times 30.0 \text{ mm}$  stilbene scintillator in another collimator situated at an angle of about  $60^\circ$ . For the neutron energy range from 1 to 5 MeV, the  $T(p,n)^3\text{He}$  reaction was used to produce monoenergetic neutrons by changing the detection angles, for 6 to 20 MeV the same reaction was used at  $0^\circ$  by changing the incident proton energies, and for 21 to 30 MeV the  $T(d,n)^3\text{He}$  reaction was chosen at  $0^\circ$  by changing the incident deuteron energies. The gas target was a gas cell with the size of  $\phi 10.0 \text{ mm} \times 30.0 \text{ mm}$ , filled with tritium gas to a pressure of 101.325 kPa. More details about the tritium gas target system can be found in Ref. [9].

First, the gamma calibration was performed before the experiment to obtain the relation between the ADC channels and electron-equivalent energy ( $E_{ee}$ ). Four sources were used for the calibration:  $^{137}\text{Cs}$ ,  $^{22}\text{Na}$ ,  $^{54}\text{Mn}$  and  $^{65}\text{Zn}$ . This calibration was performed several times during the experiment to monitor the stability of the system.

After the gamma calibration, the LS was irradiated by monoenergetic neutrons with different energies between 1 to 30 MeV. All events from the detector were recorded by a list mode with a CAMAC Data Acquisition (DAQ) system. For each event, there are three parameters which are PH, PSD and TOF. PH and PSD were used for the detection threshold determination and n- $\gamma$  discrimination. TOF was used to select the monoenergetic neutrons.

In order to reduce the deadtime of the detectors, electronics and DAQ system, the beam current was reduced to several tens of nA. The pulsed beam was

used to perform the TOF measurement, which is necessary to select the monoenergetic neutrons when the breakup channels are open for p-T and d-T reactions. For each energy, both GAS IN and GAS OUT measurements were performed to subtract the background correctly.

### 3 Data analysis and results

Before the simulation of the detection efficiency, the neutron light output and the energy dependent resolution function of the detector have to be determined first. As described in section 2 of this paper, the first step of the data analysis is to get the exact position of the Compton edges of each of the gamma resources.

#### 3.1 Determination of the energy scale according to the position of the gamma source's Compton edge

The basic principle of the data analysis for gamma calibration is the following.

- 1) Using the half maximum of the Compton edges, a rough gamma calibration result was obtained.
- 2) The PH spectra of the LS for different gamma sources were simulated by the GRESP<sup>[10]</sup> code.
- 3) The simulated spectra were folded with an energy dependent resolution function and the energy scale was adjusted according to the first calibration result from step 1.
- 4) The simulated spectra (after folding and energy scale adjustment) were fitted to the measured ones at the Compton edge region to determine the measured Compton edge. Then the new calibration result could be obtained and step 3 and step 4 could be done iteratively to improve the result. Convergence is reached if the deviations between the results of two conse-

cutive steps are within the predefined uncertainties. Fig. 2(a) shows the simulated spectrum of the  $^{137}\text{Cs}$  source compared with the measured spectrum.

### 3.2 Determination of the light output function according to the edges of the neutrons

For the neutron data, the data analysis was similar to that of the gamma calibration. First, the PH spectra for different neutron energies were simulated by the NRESP code using a default light output function as input. The NRESP and NEFF codes used in

this work have been extended to the upper limit of 50 MeV. Then the simulated spectra were folded and the energy scale was adjusted according to the result of the gamma calibration. After this, the simulated PH spectra were fitted to the measured ones at the edge region to determine the recoil proton edge. From this, a new light output function was determined and improved iteratively and fixed finally. Fig. 2(b) shows the simulated PH spectrum compared with the measured one at a neutron energy of  $E_n = 2.04$  MeV. The simulated spectrum agrees very well with the measured one.

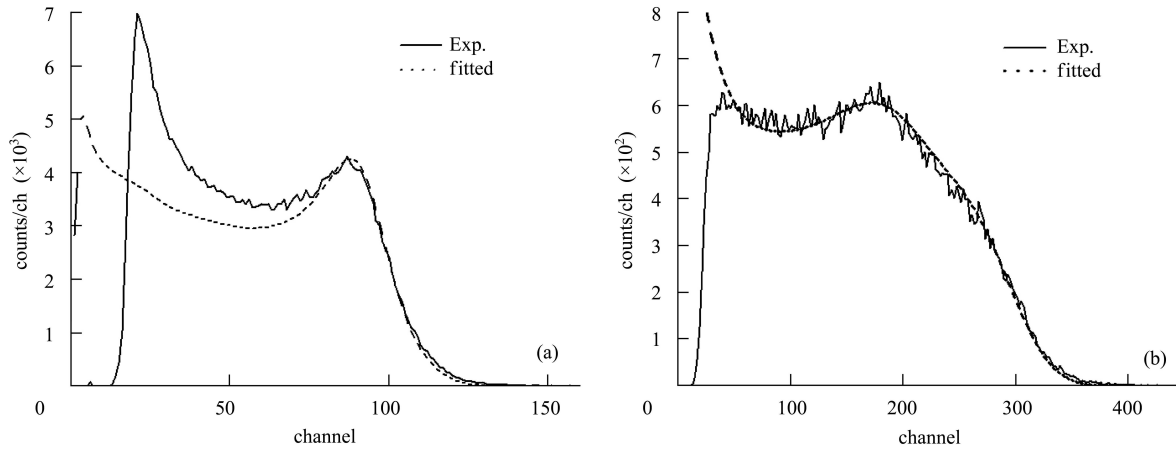


Fig. 2. Comparison of the measured and fitted PH spectra: (a) for the  $^{137}\text{Cs}$  source, (b) for the neutron at  $E_n = 2.04$  MeV.

### 3.3 Simulation of detection efficiency

According to Ref. [11], the resolution function can be described as

$$\frac{dL}{L}(E) = \sqrt{A^2 + \frac{B^2}{L} + \frac{C^2}{L^2}}, \quad (1)$$

where  $L$  is the light output of the neutron. The unit of  $L$  is called the “light unit (MeVee)” which is defined as the light output of an electron with an energy of 1 MeV.  $dL/L$  is the resolution.  $A$  is the locus-dependent light transmission from the scintillator to the photocathode.  $B$  is the statistical effect of the light production, attenuation, photon to electron conversion and electron amplification and  $C$  represents the electronic noise contribution. The resolution  $dL/L$  for each energy was obtained by folding the calculated PH spectrum with a gaussian function, and then fitted to the measured one at the edge region. The FWHM was optimized in this procedure. Finally, the  $A$ ,  $B$ ,  $C$  values were determined by a least-square fitting, and the optimal fitted resolution function was shown in Fig. 3, which roughly agrees

with the experimental one. The values of  $A=7.8\%$ ,  $B=10.6\%$  and  $C=0.5\%$  were obtained from the fitting.

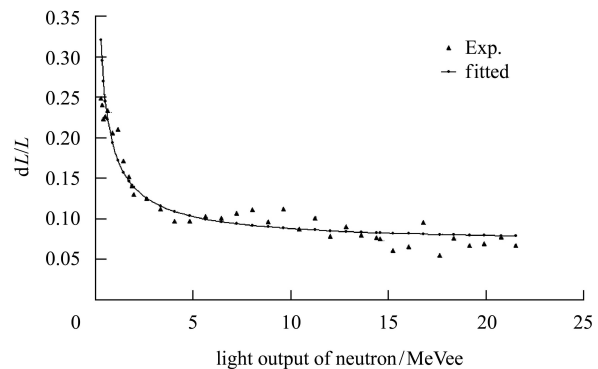


Fig. 3. The experiment-determined and fitted resolution functions.

Using the new light output function and the resolution function, the neutron response spectra and the detection efficiency were simulated with the codes of NRESP and NEFF, which have been widely used. The calculated response of the detector agrees fairly

well with the measured one below 20 MeV, mostly within an uncertainty of 3%. Above the 20 MeV region, the contribution from the  $^{12}\text{C}(n, 3\alpha)$  reaction becomes more and more significant, while the reaction cross sections and angular distributions are not known precisely enough. Therefore, the simulated response can not agree well with the measured response. The detection efficiency from the calculation also needs to be corrected.

The correction of the calculated detection efficiency was done as follows: first, the simulated PH spectra were normalized to the measured one in the recoil proton region (without influence from alpha) because the n-p scattering cross section is known very well; then, the ratios of the areas from a certain threshold to the maximum of the response spectra for measurement to the calculation can be obtained and used to correct the calculated efficiency.

In order to improve the MC calculation, it is necessary to improve the reaction cross sections and angular distributions of the  $^{12}\text{C}(n, 3\alpha)$  reaction. Since few experimental data are available above 20 MeV, this improvement can only be done roughly by comparing the measured PH spectra with the calculated ones. Firstly the contribution from the n-p scattering of measured PH spectra was subtracted by simulation, then the remaining PH spectra mainly came from the  $^{12}\text{C}(n, 3\alpha)$  reaction. The reaction cross sections for the  $^{12}\text{C}(n, 3\alpha)$  reaction used in the simulation can be improved by comparing the measurements with the calculations. Fig. 4 shows the simulation results before and after the improvement.

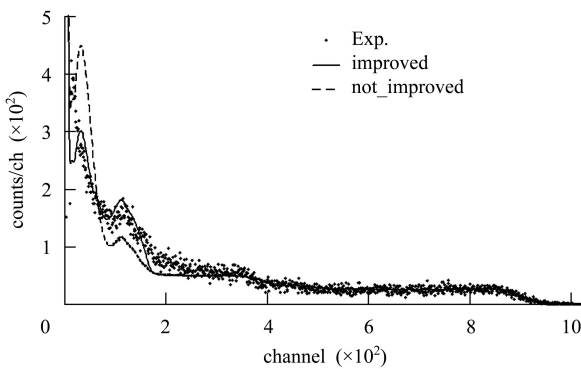


Fig. 4. Comparison of the simulated PH spectra at 30.03 MeV before and after the  $^{12}\text{C}(n, 3\alpha)$  reaction cross sections improvement.

From the procedures described above, the relative neutron detection efficiency of the liquid scintillator between 1 to 30 MeV can be obtained with an uncertainty of about 3%. Three different ways were used to verify the results obtained:

1) The relative efficiency at the near threshold region (1–5 MeV) was verified by the experimental calibration using the differential cross section angular distribution of the p-T reaction. The attenuation of the source neutrons by the gas target material at different detection angles was corrected through the MC simulation with the SINENA<sup>[12]</sup> code. Fig. 5 shows the experimental data comparing with the calculation for different detection thresholds. The threshold was defined with the Compton energy for  $^{137}\text{Cs}$  as a standard. Therefore, 1 Cs means the detection threshold is 0.477 MeV and 0.5 Cs is 0.238 MeV, and so on. One can see that the agreement is fairly well within the uncertainties. The uncertainties for the experimental data given here combine the statistics ( $\sim 1\%$ ), the uncertainty of the angular distribution of the p-T reaction ( $\leq 2\%$ ) and the normalization ( $\leq 1\%$ ).

2) The results obtained with the NRESP and NEFF code were also compared with the results obtained with another widely used MC code-SCINFUL. It is necessary to do similar corrections for the calculation results with the SCINFUL code. Fig. 6 shows the results obtained with the SCINFUL code (after correction) compared with the result obtained with the NEFF code. The agreement is also good.

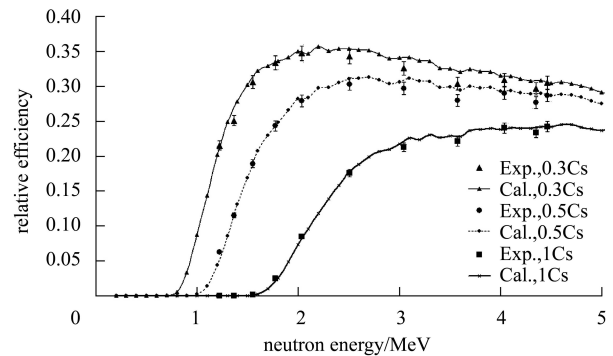


Fig. 5. Comparison between the NEFF result and the angular method's result.

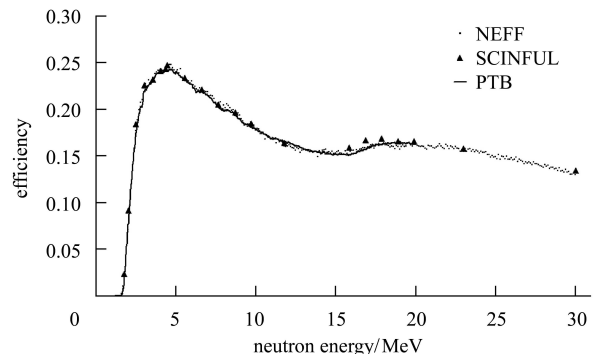


Fig. 6. Comparison between the NEFF result and the SCINFUL's result.

3) After the experiment, the detector was sent to PTB (Physikalisch Technische Bundesanstalt in Germany) to perform a similar calibration in the energy range of 1 to 14 MeV, and the detection efficiency was absolutely calibrated at 8, 10, 12 and 14 MeV with a PRT. Fig. 6 shows the results obtained at PTB compared with the results obtained at CIAE. Good agreement has been obtained.

## 4 Summary

The light output function and the neutron detec-

tion efficiency for a  $\phi 50.8 \text{ mm} \times 50.8 \text{ mm}$  BC501A scintillation detector in the energy range of 1—30 MeV was calibrated with an uncertainty of about 3%. The extended NEFF and NRESP codes were first used in the neutron detection calibration at above 20 MeV, and verified by the experiment. The  $^{12}\text{C}(n, 3\alpha)$  reaction cross sections used in the NRESP and NEFF codes were improved. The calibration results have been verified by various cross checks to improve the reliability and accuracy of the result. This work will greatly improve our capability of neutron detection in the future.

---

## References

- 1 BYRD R C, SAILOR W C. Nucl. Instrum. Methods A, 1989, **274**: 494
- 2 MEIGO S. Nucl. Instrum. Methods A, 1997, **401**: 365
- 3 FOWLER J L et al. Nucl. Instrum. Methods A, 1980, **175**: 449
- 4 DEBEVEC P T. Nucl. Instrum. Methods A, 1979, **166**: 467—471
- 5 NORIAKI NAKAO. Nucl. Instrum. Methods A, 2001, **463**: 275
- 6 DICKENS J K. ORNL report, 1998, ORNL-6463
- 7 DIETZE G et al. PTB report, 1982, **PTB-ND-22**: 1
- 8 SA Jun. Atomic Energy Science and Technology, 1992, **26**: 1 (in Chinese)
- 9 QI BUJIA. Qingdao University Transactions, 1997, **10**: 86 (in Chinese)
- 10 DIETZE G, KLEIN H. Nucl. Instrum. Methods A, 1982, **193**: 549
- 11 MILOS TICHY et al. PTB Report, 1992, **PTB-7.2-92-1**: 26
- 12 SCHMIDT D et al. PTB Report, 2000, **PTB-N-40**: 1